

MWRRETV2 Value-Added Product Report: The Retrieval of Liquid Water Path and Precipitable Water Vapor from Microwave Radiometer – 3-Channel (MWR3C) Data Sets

D Zhang
KL Gaustad

LD Riihimaki
DD Turner

May 2020



DISCLAIMER

This report was prepared as an account of work sponsored by the U.S. Government. Neither the United States nor any agency thereof, nor any of their employees, makes any warranty, express or implied, or assumes any legal liability or responsibility for the accuracy, completeness, or usefulness of any information, apparatus, product, or process disclosed, or represents that its use would not infringe privately owned rights. Reference herein to any specific commercial product, process, or service by trade name, trademark, manufacturer, or otherwise, does not necessarily constitute or imply its endorsement, recommendation, or favoring by the U.S. Government or any agency thereof. The views and opinions of authors expressed herein do not necessarily state or reflect those of the U.S. Government or any agency thereof.

MWRRETV2 Value-Added Product Report: The Retrieval of Liquid Water Path and Precipitable Water Vapor from Microwave Radiometer – 3-Channel (MWR3C) Data Sets

D Zhang, Pacific Northwest National Laboratory

LD Riihimaki, Cooperative Institute for Research in Environmental
Sciences

KL Gaustad, Pacific Northwest National Laboratory

DD Turner, National Oceanic and Atmospheric Administration Earth
System Research Laboratory

May 2020

Work supported by the U.S. Department of Energy,
Office of Science, Office of Biological and Environmental Research

Executive Summary

This report provides a short description of the U.S. Department of Energy Atmospheric Radiation Measurement (ARM) user facility Microwave Radiometer – 3-Channel (MWR3C) Retrieval (MWRRETV2) Value-Added Product (VAP) algorithm. MWRRETV2 is an updated version of MWRRET, which extends the physical-iterative retrieval of liquid water path (LWP) and precipitable water vapor PWV) to 3-channel microwave radiometers beyond ARM's original standard 2-channel (23-and 31-GHz) systems. The 89-GHz channel in the 3-channel microwave radiometers has approximately three times the sensitivity to liquid water as the 31-GHz channel, thus improving LWP retrieval accuracy when LWP is less than 100 g/m². We present a general overview of the technique, input parameters, and output products, and describe data quality checks.

Acknowledgments

Many thanks to Carolyn Brauer for providing the brightness temperature residue plot and manual monthly brightness temperature bias at ARM's Eastern North Atlantic (ENA) site, and to Maximillian Maahn for providing manual monthly brightness temperature bias at ARM's North Slope of Alaska (NSA) Oliktok Point site

Acronyms and Abbreviations

AGL	above ground level
AMF	ARM Mobile Facility
ARM	Atmospheric Radiation Measurement
ARRA	American Recovery and Reinvestment Act
ARSCL	Active Remote Sensing of Clouds Value-Added Product
ENA	Eastern North Atlantic
LWP	liquid water path
MWR	microwave radiometer
MWR3C	microwave radiometer – 3-channel
MWRRET	Microwave Radiometer Retrieval
MWRRETV2	Microwave Radiometer Retrieval Version 2
NSA	North Slope of Alaska
PWV	precipitable water vapor
QC	quality control
RH	relative humidity
SGP	Southern Great Plains
TWP	Tropical Western Pacific
VAP	value-added product

Contents

Executive Summary	iii
Acknowledgments.....	iv
Acronyms and Abbreviations	v
1.0 Introduction	1
2.0 Input Data	1
3.0 Brightness Temperature (T_b) Offsets.....	2
4.0 Data Quality Testing.....	5
5.0 Output Data	6
6.0 Examples	6
7.0 Conclusions	8
8.0 References	9

Figures

1 Brightness temperature residuals (ΔT_b) recorded at the ENA site in 2017.	2
2 Comparison of mean T_b bias at the three frequencies from the automated technique with manual monthly T_b bias at the ENA site (Carolyn).....	3
3 Comparisons of mean T_b bias at the three frequencies from the automated technique with manual monthly T_b bias at the Oliktok point (Max).	4
4 Histograms of clear-sky T_b residuals at the 23.8, 30, and 89-GHz channels retrieved from the ENA site in 2017.	5
5 Quicklook image of MWR3C measurements and retrieved LWP and PWV on 8 February 2018 at Oliktok Point.	7
6 Quicklook image of MWR3C measurements and retrieved LWP and PWV on 22 August 2019 at the SGP C1 site.....	8

1.0 Introduction

Liquid water path (LWP) and precipitable water vapor (PWV) are geophysical variables used by a large number of the U.S. Department of Energy Atmospheric Radiation Measurement (ARM) user facility data users. These variables are typically retrieved from microwave radiometers (MWRs) using a statistical methodology based on site-dependent monthly retrieval coefficients (Liljegren and Lesht 1996). Historically, the standard ARM radiometers were 2-channel systems (23.8 and 31.4 GHz) that give an uncertainty in the retrieved LWP of approximately 25 g/m² (Turner et al. 2007). With American Recovery and Reinvestment Act (ARRA) funding, new 3-channel systems (23.8, 30, 89 GHz) have been installed at the Southern Great Plains (SGP) central and extended facility sites, the Tropical Western Pacific (TWP) Manus and Darwin sites, the Eastern North Atlantic (ENA) site, and as part of the ARM Mobile Facilities (AMF). These new MWRs are described by Cadeddu et al. (2013). The 89-GHz channel has approximately three times the sensitivity to liquid water as the 31.4-GHz channel and will therefore markedly improve the accuracy of the LWP when LWP is less than 100 g/m² (Löhnert and Crewell 2003). Since the median LWP at all the ARM observatories is less than 100 g/m², this improvement is greatly desired (Turner et al. 2007).

The original retrieval algorithm (MWRRET), as described in Turner et al. (2007) and Gaustad et al. (2011), uses a physical-iterative method to improve PWV and LWP retrievals. MWRRET was designed specifically for the 2-channel systems and includes a significant amount of quality controls (QC) for those systems, including an adaptive correction for brightness temperature (T_b) offsets that may change over time; thus, it cannot be applied to the 3-channel systems. The new MWRRETV2 value-added product (VAP) is based on code that extends the physical-iterative retrieval algorithm to be more flexible so that it can work with any set of two or more microwave frequencies to retrieve PWV and LWP. The goal of this VAP is to run PWV and LWP retrievals on MWR3C measurements routinely. Details of the physical-iterative retrieval algorithm are elaborated in Turner et al. (2007). We refer readers to this article for more information about the algorithm. Additionally, the new algorithm will use an updated version of the radiative transfer model (MonoRTM v4.2), which has significant changes to the water vapor continuum, water vapor line parameters (i.e., spectral widths), and nitrogen continuum (Turner et al. 2009, Cadeddu and Turner 2011).

2.0 Input Data

Required inputs for this VAP are microwave brightness temperatures and atmospheric profile (temperature, pressure, humidity) information. The input microwave brightness temperatures come from the mwr3c.b1 datastream, which is the datastream with basic QC checks applied to MWR3C radiometer measurements. The MWR3C configuration and its calibration are provided in the ARM MWR3C Instrument Handbook (https://www.arm.gov/publications/tech_reports/handbooks/mwr3c_handbook.pdf). For each radiometer channel used in the VAP, the field_name, frequency, and 1-sigma uncertainty on the brightness temperature values must be specified.

The atmospheric profile comes from ARM radiosonde files. The code reads all of the radiosonde data for the current, previous, and next days; does basic quality control checks; and interpolates the sondes to a common height grid. Then, for each MWR sample time, the atmospheric profile is interpolated to that time.

Optional inputs include cloud base height and precipitation from surface meteorological system data. The cloud base and top heights will preferentially come from the Active Remote Sensing of Clouds ([ARSCL](#)) cloud boundary value-added product. If ARSCL is not available, the ceilometer cloud base height will be used, and the cloud will be assumed to have a default thickness. If ceilometer cloud base height is not available, then the atmospheric profile will be searched for high-relative-humidity layers to use as cloud base. If no layers with high relative humidity (RH) are found, a cloud base of 1 km above ground level (AGL) will be assumed. The cloud temperature will be set as the mean temperature of the profile between the cloud base and top heights. The cloud base and top heights used in the retrieval and a variable indicating the source of the cloud base and top height information will be output.

Surface meteorological system data provide precipitation data for flagging cases where the retrieval is indeterminate or bad. The input precipitation field will be gridded to the radiometer time samples using nearest-neighbor interpolation.

3.0 Brightness Temperature (T_b) Offsets

Systematic biases in the brightness temperature measurements, however, could lead to errors in the retrieved LWP. Meijgaard and Crewell (2005) showed that the retrieved LWP from microwave radiometer measurements is significantly nonzero in clear-sky conditions and suggested that the T_b offsets need to be determined and subtracted via postprocessing to yield close-to-zero LWP.

Traditionally, manual T_b offsets at 23.8 GHz and 31.4 GHz were done annually for the 2-channel MWR systems – MWRRET VAP (https://www.arm.gov/publications/tech_reports/doe-sc-arm-tr-081.2.pdf). Recently, we have shown that correcting bias on a shorter timescale (monthly) can improve the data quality by having the ability to account for drifts and data anomalies. This is demonstrated in Figure 1, which shows brightness temperature residuals ($\Delta T_b = T_b(\text{obs}) - T_b(\text{calc})$) recorded on each frequency channel of the MWR3C during clear-sky periods at the ENA site in 2017 as a function of time. The uncorrected values are shown in the left panel, values corrected on an annual basis using a single bias correction for each channel are shown in the middle panel, and values corrected on a monthly basis are in the right panel. The clear upward trend evident in the uncorrected data from the 89-GHz channel persists in the annually corrected data but is not seen in the monthly corrections.

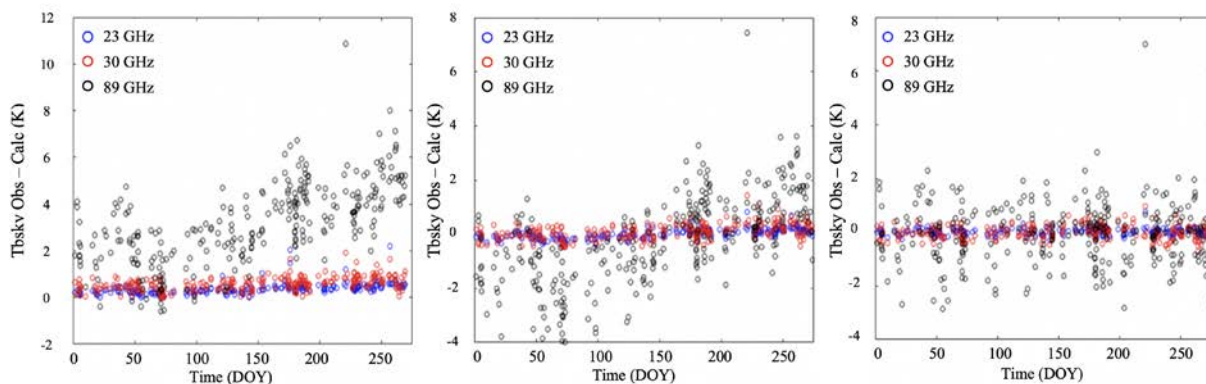


Figure 1. Brightness temperature residuals (ΔT_b) recorded at the ENA site in 2017. Uncorrected values are shown in the left panel, annually corrected value (based on a single set of bias offsets for the entire year) are in the middle panel, and monthly corrected values are in the right panel.

This method can be time consuming and labor intensive. Since natural data do not necessarily adhere to a human timeline, corrections may not be representative of the true bias. To mitigate these challenges, we developed an automated T_b bias correction process on a rolling 60 days-or-longer window depending on the available amount of clear-sky measurements at each site. For example, for SGP sites and the Oliktok point site, a 60-day rolling window is used; for the ENA site, a 90-day rolling window is used because the ENA site is often covered by low-level marine stratocumulus.

The T_b residual in clear-sky conditions at each frequency channel is defined as:

$$\Delta T_b(\nu) = \text{tbsky_obs}(\nu) - \text{tbsky_calc_cs}(\nu) \tag{1}$$

where $\text{tbsky_obs}(\nu)$ is the instantaneous observed brightness temperature at frequency channel ν (23, 30, or 89 GHz) and $\text{tbsky_calc_cs}(\nu)$ is the clear-sky calculated brightness temperature.

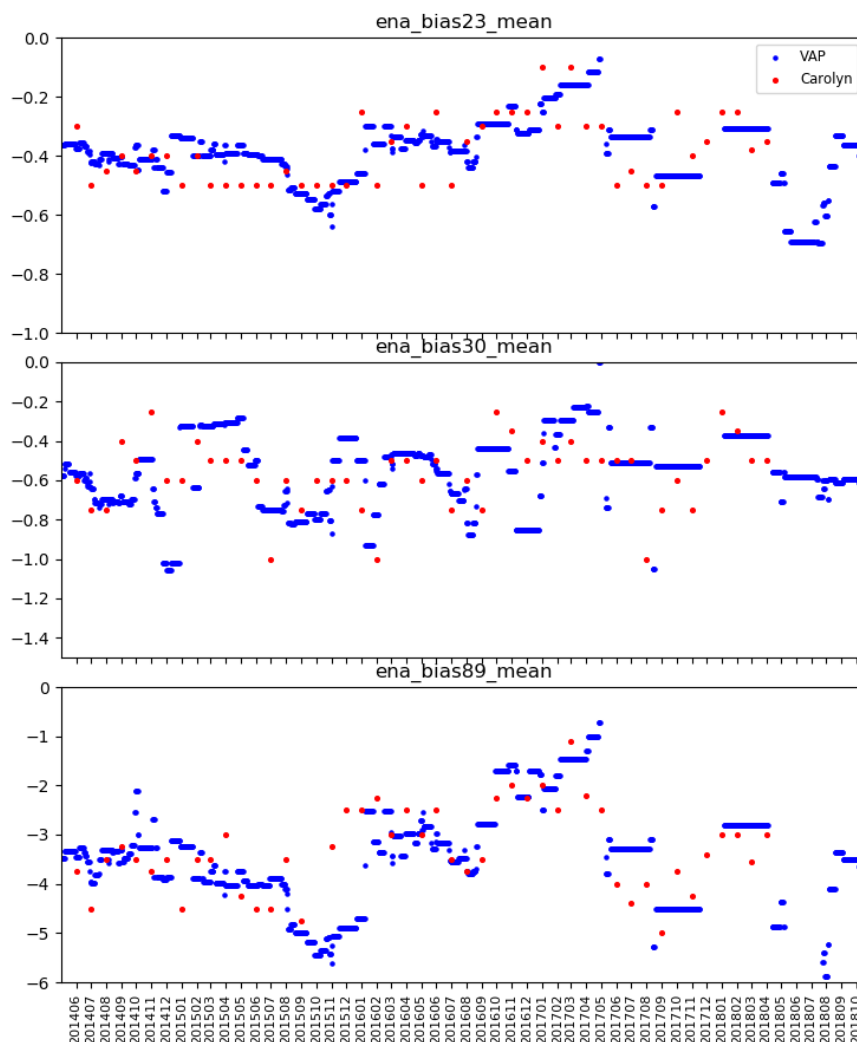


Figure 2. Comparison of mean T_b bias at the three frequencies from the automated technique with manual monthly T_b bias at the ENA site (Carolyn).

To be considered clear sky, two conditions must be met: 1) no cloud is detected by active remote-sensing measurements ($cbh_detected \leq 0$), and 2) the standard deviation of T_b over a defined temporal window (usually 20 minutes) must be below a predetermined threshold, which is a function of the PWV. For each site, a plot of the standard deviation of T_b at 30 GHz versus physical PWV is made to which a line is fit (polynomial or smaller degree). The threshold is determined by the quadratic equation given in Equation 2.

$$\text{threshold} = c + a*(PWV)^1 + b*(PWV)^2 \tag{2}$$

c, a, b are constants. For SGP sites and the ENA site, c, a, b are 0.3, -0.01, and 0.004, respectively; for the Oliktok point, they are 0.6, 0.0, and 0.0, respectively.

To validate the automated T_b bias determination technique, Figures 2 and 3 show the comparisons of mean T_b bias from the automated technique with manual monthly T_b bias at the ENA site (by Carolyn Brauer, labeled as ‘Carolyn’) and Oliktok point (by Maximilian Maahn, labeled as ‘Max’).

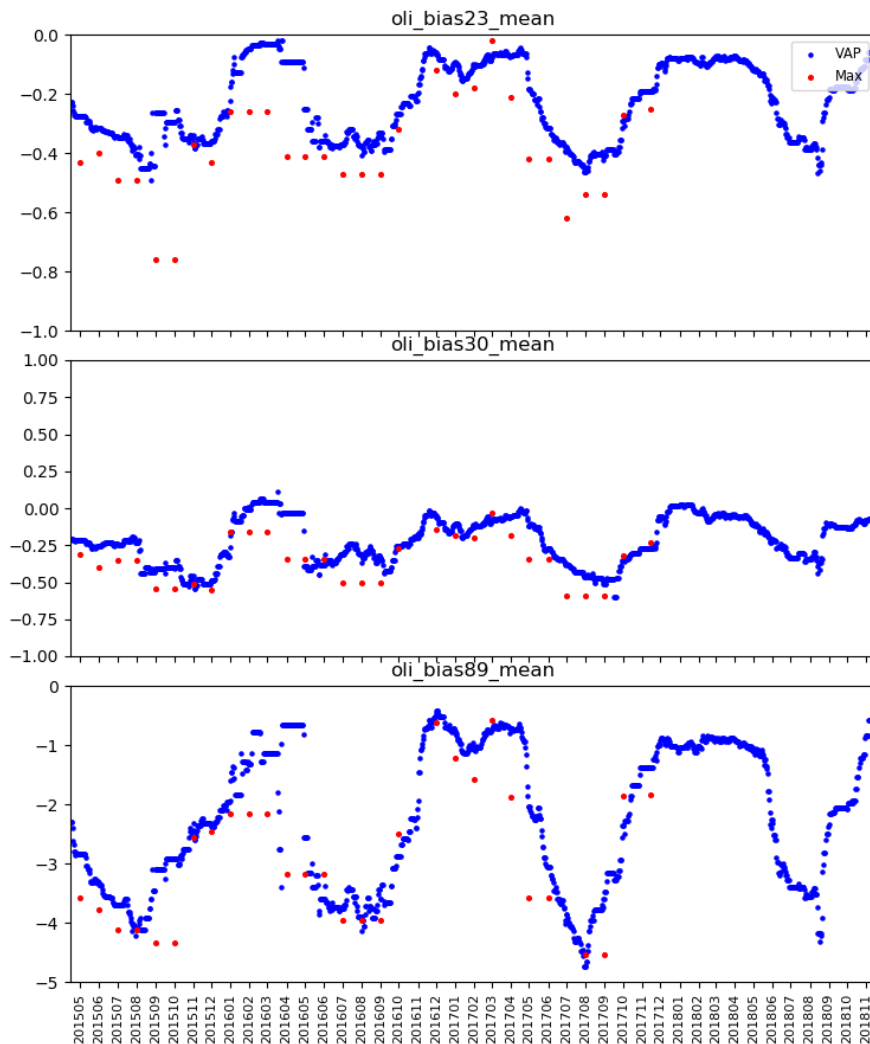


Figure 3. Comparisons of mean T_b bias at the three frequencies from the automated technique with manual monthly T_b bias at the Oliktok Point site (Max).

Histograms of $\Delta T_b(\nu)$ from Equation 1 that meet the clear-sky conditions, elevation angle, and QC flag criteria are made for each of the frequency channels. An example is shown in Figure 4, which shows $\Delta T_b(\nu)$ for data recorded in 2017 at the ENA site.

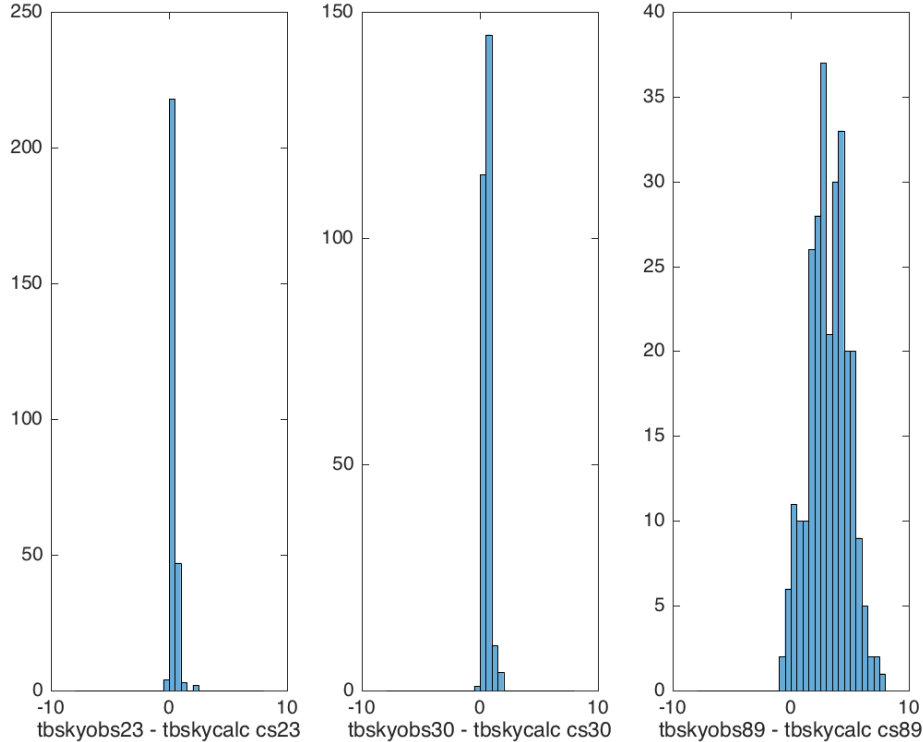


Figure 4. Histograms of clear-sky T_b residuals at the 23.8, 30, and 89-GHz channels retrieved from the ENA site in 2017.

The mean and standard deviations of $\Delta T_b(\nu)$ are calculated for the time window size that has been determined appropriate for a given site and the values of mean $\Delta T_b(\nu)$ provide the bias offsets, which are used to correct $T_b(\nu)$ and improve LWP and PWV retrievals.

4.0 Data Quality Testing

All quality flags associated with the input fields are propagated to the output. A QC flag is set for each retrieved variable to indicate whether the retrieval is good or bad. Quality control tests applied include identification of unrealistic retrievals ($PWV < 0$), number of iterations of retrievals, and standard deviations of outputs. In addition, a variable ‘converged’ is set to indicate if the physical-iterative retrievals of PWV and LWP are converged or not. Another variable ‘num_iteration’ is used to store the number of iterations performed by the retrieval.

5.0 Output Data

The primary geophysical output variables are estimates of the PWV and LWP along with 1-sigma uncertainties and quality flags on the calculated values.

Secondary output variables include information used in the retrieval such as input brightness temperatures, cloud base height, cloud top height, cloud temperature, and source of cloud base/top information. The output file will also include variables that characterize the quality of the retrieval such as the number of iterations performed in the retrieval and the root-mean-square difference between observed and final computed brightness temperatures.

Flags that indicate clear-sky and precipitating periods will also be included in the output.

One file is created for each day named with the following convention:

XXXmwrret2turnFF.c1.YYYYMMDD.hhmmss

where:

XXX = the location of the instrument (nsa, sgp, ena, oli, etc.)

mwrret2turn = identifies that this is WMRRETv2 VAP

FF = facility (e.g., C1)

YYYYMMDD = year, month, and day

hhmmss = hour, minute, second

The VAP generates a quicklook output file within which four plots are presented: (1) MWR3C brightness temperature values at three frequencies, (2) PWV calculated by the statistical ('stat') and physical-iterative ('phys') retrieval methods, (3) LWP calculated by the 'stat' and 'phys' retrieval methods, and (4) surface temperature or rain intensity. Two versions of this quicklook product are created. One version has a standard fixed y-axis for each of the plots, and another a dynamically resized y-axis to automatically adjust for periods with relatively flat brightness temperature and retrieval values. The output file for the standard and dynamically resized quicklook uses the following naming convention:

XXXmwrret2turnFF.YYYYMMDD.png

XXXmwrret2turnFF.YYYYMMDD.dynamic.png.

6.0 Examples

Figure 3 demonstrates the dynamically resized quicklook product for 8 February 2018 at Oliktok Point. The top panel shows the MWR3C measured brightness temperatures at 23.8 (blue), 30 (red), and 89 GHz (green). The calculated clear-sky brightness temperatures are also plotted as large dots. The middle two panels show the retrieved PWV and LWP using the physically iterative method ('physpwv' and 'physlwp', blue lines) and statistical method ('statpwv' and 'satlwp', green lines). Physically iterative retrievals that are not converged are also plotted (red lines). A case on 22 August 2019 at the SGP C1 site is demonstrated in Figure 4, which shows significant amounts of physically iterative retrievals that are not converged. The bottom panel shows the measured surface temperature (Figure 5) or rain intensity (Figure 6).

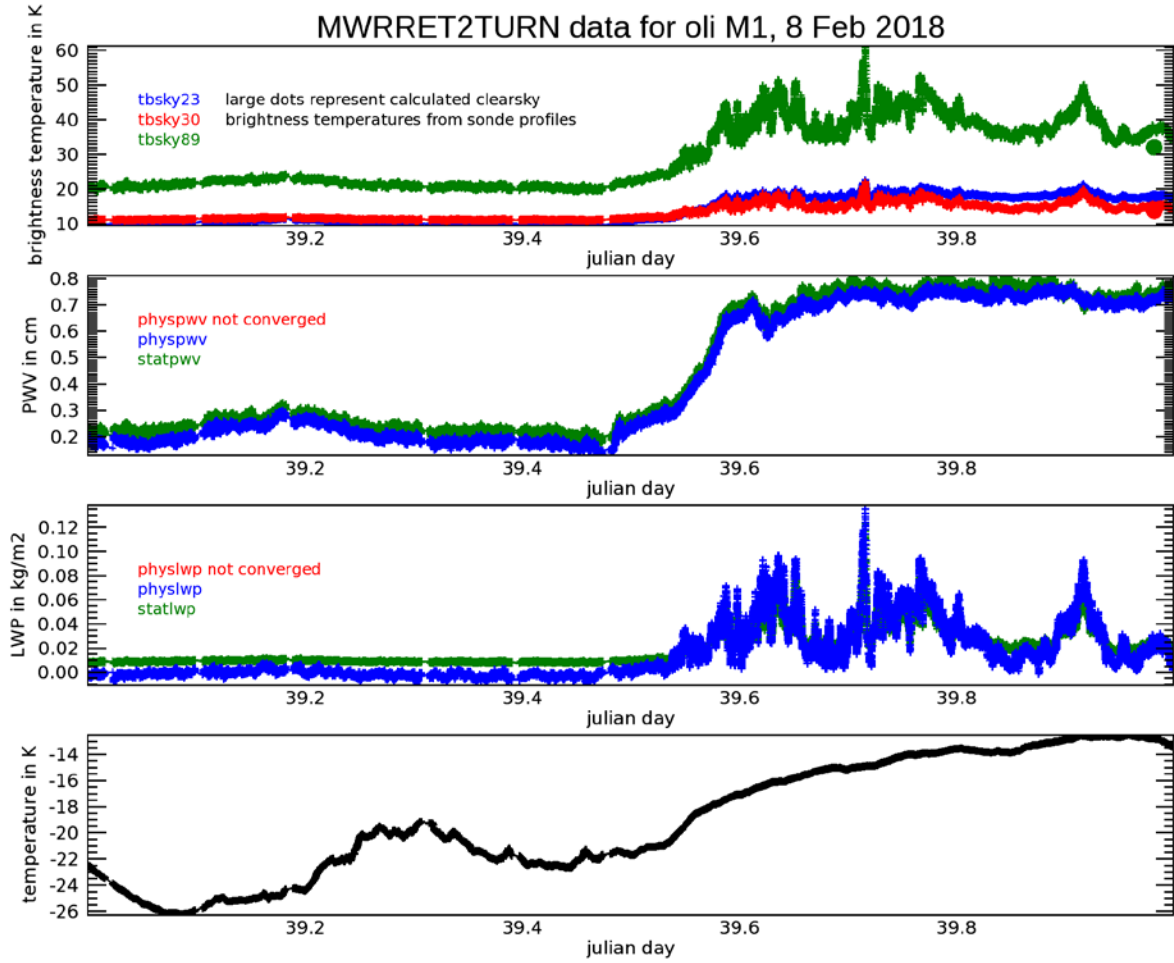


Figure 5. Quicklook image of MWR3C measurements and retrieved LWP and PWV on 8 February 2018 at Oliktok Point.

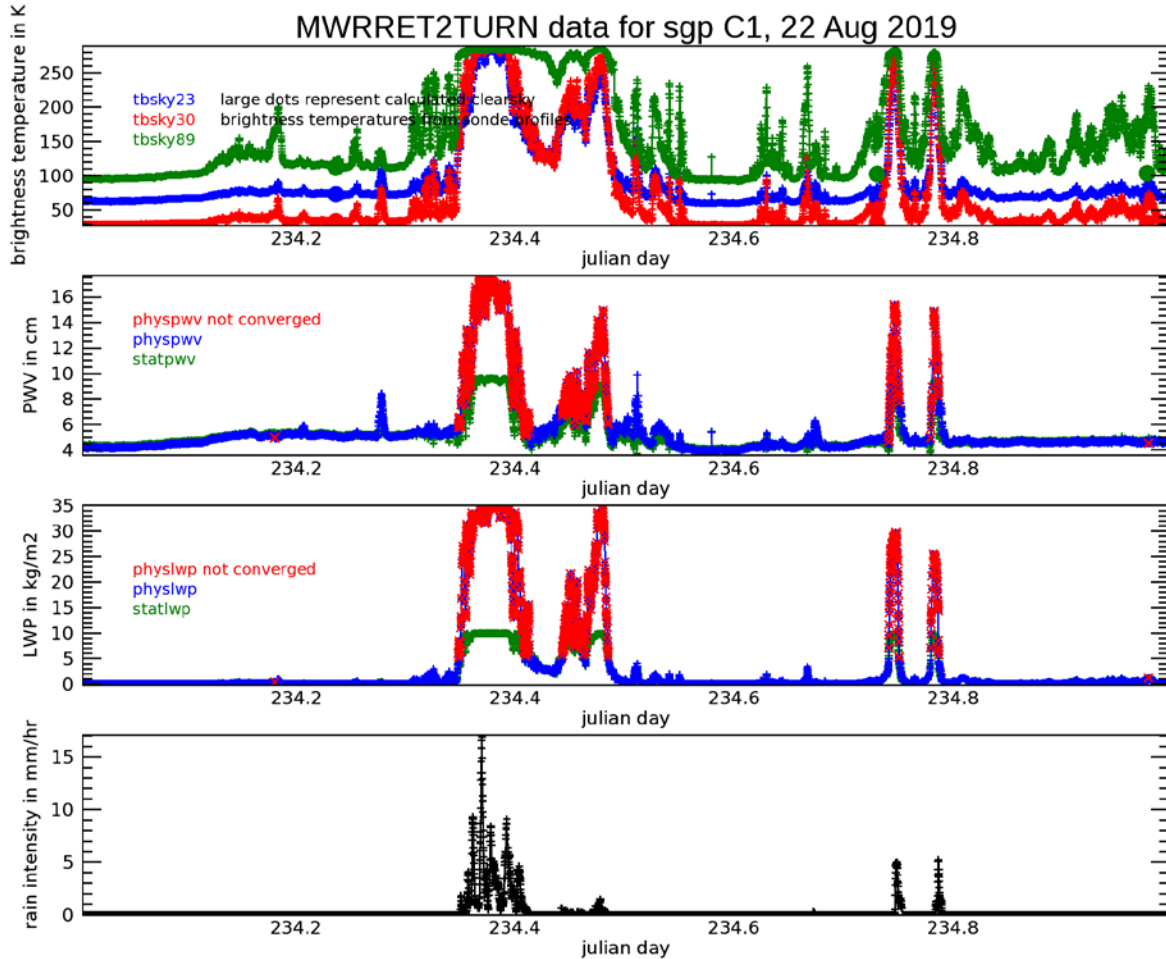


Figure 6. Quicklook image of MWR3C measurements and retrieved LWP and PWV on 22 August 2019 at the SGP C1 site.

7.0 Conclusions

The 3-channel microwave radiometer (MWR3C) provides radiation measurements at 23.8, 30, and 89 GHz, which can be used to retrieve atmospheric precipitable water vapor and liquid water path. Compared to the traditional 2-channel MWR measurement at 23.8 and 30 GHz, the 89-GHz channel in the 3-channel microwave radiometers has approximately three times the sensitivity to liquid water as the 31-GHz channel, thus improving LWP accuracy when LWP is less than 100 g/m^2 . We extend the physical-iterative retrieval algorithm to be more flexible to work for the MWR3C measurements. The new algorithm also uses an updated version of the radiative transfer model (MonoRTM v4.2). The PWV and LWP retrievals provided by MWRRETV2 are critical to understanding low-liquid-containing clouds such as shallow continental cumulus at the SGP site and polar mixed-phase clouds at the NSA site.

8.0 References

- Cadeddu, MP, and DD Turner. 2011. "Evaluation of water permittivity models from ground-based observations of cold clouds at frequencies between 23 and 170 GHz." *IEEE Transactions on Geoscience and Remote Sensing* 49(8): 2999–3008, <https://doi.org/10.1109/TGRS.2011.2121074>
- Cadeddu, MP, JC Liljegren, and DD Turner. 2013. "The Atmospheric Radiation Measurement (ARM) program network of microwave radiometers: Instrumentation, data, and retrievals." *Atmospheric Measurement Techniques* 6(9): 2359-2372, <https://doi.org/10.5194/amt-6-2359-2013>
- Gaustad, KL, DD Turner, and SA McFarlane. 2011. MWRRET Value-Added Product: The Retrieval of Liquid Water Path and Precipitable Water Vapor from Microwave Radiometer (MWR) Data Sets. U.S. Department of Energy. [DOE/SC-ARM-TR-081.2](https://doi.org/10.1109/DOE/SC-ARM-TR-081.2).
- Liljegren, JC, and BM Lesht. 1996. "Measurements of integrated water vapor and cloud liquid water from microwave radiometers at the DOE ARM cloud and radiation testbed in the U.S. Southern Great Plains." In *IGARSS '96. International Geoscience and Remote Sensing Symposium 3*: 1675–1677, [doi:10.1109/IGARSS.1996.516767](https://doi.org/10.1109/IGARSS.1996.516767).
- Löhnert, U, and S Crewell. 2003. "Accuracy of cloud liquid water path from ground-based microwave radiometry 1. Dependency on cloud model statistics." *Radio Science* 38(3): 8041, <https://doi.org/10.1029/2002RS002654>
- van Meijgaard, E and S. Crewell. 2005. "Comparison of model-predicted liquid water path with ground-based measurements during CLIWA-NET." *Atmospheric Research* 75(3): 201–226, <https://doi.org/10.1016/j.atmosres.2004.12.006>
- Turner, DD, SA Clough, JC Liljegren, EE Clothiaux, KE Cady-Pereira, and KL Gaustad. 2007. "Retrieving liquid water path and precipitable water vapor from Atmospheric Radiation Measurement (ARM) microwave radiometers." *IEEE Transactions on Geoscience and Remote Sensing* 45(11): 3680–3690, <https://doi.org/10.1109/TGRS.2007.903703>
- Turner, DD, U Loehnert, M Cadeddu, S Crewell, and A Vogelmann. 2009. "Modifications to the water vapor continuum in the microwave suggested by ground-based 150 GHz observations." *IEEE Transactions on Geoscience and Remote Sensing* 47(10): 3326–3337, <https://doi.org/10.1109/TGRS.2009.202262>



U.S. DEPARTMENT OF
ENERGY

Office of Science